

RESEARCH

Open Access



3' UTR is critical for viral RNA accumulation of jasmine virus H

Li-Juan Zhu^{1†}, Chong-Tao Zhang^{2†}, Ya-Ni Bai¹, Chao-Yang Jiang¹, Shi-Yun He², Qing Chang¹, Qian Xu¹ and Yan-Hong Han^{1*} 

Abstract

Jasmine virus H (JaVH) is a newly reported viral pathogen of jasmine in China and USA. To study the viral gene function and pathogenic mechanism, a full-length infectious clone of JaVH (pXT-JaVH^{FJ}) was constructed under the control of the cauliflower mosaic virus 35S promoter. pXT-JaVH^{FJ} induced a systemic infection in *Nicotiana benthamiana* plants by Agro-infiltration, which demonstrated that pXT-JaVH^{FJ} was biologically active. Jasmine showed yellow spots after rubbing with total RNA extracted from Agro-infiltrated *N. benthamiana*, indicating that JaVH was highly associated with yellow mosaic symptoms observed on jasmine. To investigate the occurrence and mutations of the virus, jasmine samples were collected from eight provinces of China and were tested for JaVH. The samples that were tested positive for JaVH were used to determine the complete genome sequences. They were comprised of 3867 or 3868 nucleotides and their genome organizations resembled that we previously reported for JaVH-FJ. Phylogenetic analyses and sequence comparisons suggest that the eight virus isolates were close isolates of JaVH-FJ and the isolate from Jilin Province was most closely related to JaVH-FJ with 99.2% nucleotide identity over the entire genome and 99.7% identity of coat protein. Further comparative analyses of JaVH-FJ and JaVH-JL revealed additional nucleotide differences in the 3'-untranslated region (3' UTR). An infectious clone of JaVH-JL and chimeric mutants containing JaVH-FJ or JaVH-JL 3' UTRs were then constructed for further study. The differential accumulation of JaVH with distinct 3' UTR suggested that the 3' UTR of JaVH plays a crucial role in viral RNA accumulation.

Keywords Jasmine virus H, Infectious clone, siRNA, Genetic diversity, 3' UTR

Background

Jasmine (*Jasminum sambac* (L.) Aiton) belongs to the family Oleaceae and is endowed with a wide repertoire of potential uses. Jasmine is cultivated as an important cash crop and of great cultural value in China. Jasmine plants generally exhibit chlorotic mosaicism on their

leaves, which is believed to be the consequence of viral infection. Jasmine virus H (JaVH) is a new member of the *Pelarspovirus* genus in the *Tombusviridae* family that was found in the infected jasmine in Fujian Province of China (Zhuo et al. 2018), Washington, D.C., and Hawaii of USA (Dey et al. 2018). JaVH has been proved to be chlorotic associated in Jasmine leaves. JaVH is a (+)-strand RNA virus that is neither 5'-capped nor 3'-polyadenylated. The monopartite genome consists of 3867 nucleotides (nts), encoding five open reading frames (ORFs) that include replication proteins p27 and p87, movement proteins MP1 and MP2, and coat protein (CP) p37 (Zhuo et al. 2018). The genome is flanked by a short untranslated region (UTR) of 19 nts at the 5' end and a 226 nts long UTR at the 3' end (Zhuo et al. 2018).

[†]Li-Juan Zhu and Chong-Tao Zhang contributed equally to this work.

*Correspondence:

Yan-Hong Han
yan-hong@fafu.edu.cn

¹ Vector-Borne Virus Research Center, College of Plant Protection, Fujian Agriculture and Forestry University, Fuzhou 350002, China

² College of Life Sciences, Fujian Agriculture and Forestry University, Fuzhou 350002, China



Genomic RNA (gRNA) of pelarspoviruses directly translates the two replication proteins, whereas CP and two movement proteins are translated from one subgenomic RNA (sgRNA) (Castaño et al. 2009; Scheets et al. 2015). The CPs in this genus not only functions in RNA packaging, but also functions as a viral suppressor of RNA silencing (VSR). For instance, the p37 of pelargonium line pattern virus (PLPV) exerts its VSR function by sequestering small RNAs (Pérez-Cañamás and Hernández 2015, 2018). Using the *Agrobacterium* co-infiltration transient expression system, the p37 of JaVH was shown to effectively suppress the activity of RNA silencing in *Nicotiana benthamiana*, which proved its role as a VSR (Zhu et al. 2022).

Many plant RNA viruses offset the lack of both 5'-cap and 3'-poly (A) tail structures by forming long-distance RNA–RNA interactions (LDRIs) to translate, which employs a cap-independent translational enhancers (CITEs) in the 3' UTR (Dreher and Miller 2006; Kneller et al. 2006; Nicholson and White 2011; Firth and Brierley 2012). LDRIs are typical terminal modifications required for efficient initiation of translation (Fabian and White 2004), which contributes significantly to the control of genome replication, translation initiation, translational recoding, and sgRNA transcription (Jiang et al. 2010). Studies of the pelarspovirus, PLPV, have highlighted the key role of long-distance kissing-loop interactions between the 3'-CITE and 5'-proximal hairpins for gRNA and sgRNA translation (Blanco-Pérez et al. 2016). A form of 3'-CITE, named translation enhancer domain (TED)-like CITE, has been identified (Simon and Miller 2013; Simon 2015) and are conservative among all pelarspoviruses (Blanco-Pérez et al. 2016).

Central elements, such as Pr loop, tRNA-shaped structure (TSS), and H4 in the 3' UTR of turnip crinkle virus (TCV), regulate viral translation and replication (Yuan et al. 2012). A Y-shaped RNA structure in the 3' UTR of red clover necrotic mosaic virus RNA2 has been identified as a novel element required for RNA2 replication (An et al. 2010). A single-nucleotide substitution in the 3' UTR of beet black scorch virus significantly increased its viral pathogenicity (Xu et al. 2012). A small RNA hairpin known as sHP in the 3' UTR of dengue virus is found

to be critical for viral replication in cells (Nicholson and White 2014).

In this study, we generated an infectious clone of JaVH-FJ and detected the infectivity in *N. benthamiana* and *J. sambac* plants. The characterization of virus-derived small RNAs from original jasmine plants and experimentally infected *N. benthamiana* plants indicated that JaVH triggers host RNA silencing-mediated antiviral immunity. Additionally, we analyzed the eight JaVH full-genomes in the isolates that were collected from naturally infected jasmine plants in different provinces of China, where they display high genetic variability. An infectious clone of JaVH-JL and chimeric mutants on the basis of differences between JaVH-JL and JaVH-FJ were constructed and we found that the 3' UTRs of JaVH play a vital role in the process of viral infection. The results uncovered the existence of antiviral RNA silencing in jasmine plants and the critical role of the JaVH 3' UTR in viral RNA accumulation.

Results

Generation of an infectious clone of JaVH

An infectious clone of JaVH, pXT-JaVH^{FJ} (Fig. 1a), was constructed by inserting the PCR-amplified full-length JaVH into the *Stu* I and *Bam* H I digested vector pCB301 (Yao et al. 2011). The plasmid was then transformed into *Agrobacterium tumefaciens* GV3101 by Agrobacterium infiltration, as previously described (Han et al. 2010). At 7 days post-infiltration (dpi) with pXT-JaVH^{FJ}, systemic leaves of *N. benthamiana* were collected. Unlike the mosaic symptoms presented on jasmine leaves in the field, no obvious symptoms were observed on the leaves of *N. benthamiana* (Fig. 1b). Nevertheless, a viral genomic RNA and viral derived small RNAs of the expected size were detected in *N. benthamiana* leaves that were infected with pXT-JaVH^{FJ} (Fig. 1c). Members of the genera *Pelarspovirus* and *Carmovirus* are closely related viruses, but they can be distinguished by the number of sgRNAs (Scheets et al. 2015). Only one sgRNA was detected by Northern blotting, which further verified our previous prediction of JaVH as a pelarspovirus (Zhuo et al. 2018). To determine the start site of the sgRNA, we performed 5' RACE experiments

(See figure on next page.)

Fig. 1 Molecular characterization of JaVH infectious clone. **a** Schematic representation of the infectious viral clone generated in the pXT binary vector. The PCR-amplified full-length of JaVH-FJ was inserted into *Stu* I and *Bam* H I digested binary vector. Open reading frames were identified in silico after sequencing of the full virus genome. Proteins are named according to homologous proteins in other pelarspoviruses. Predicted start and stop codons are indicated. Positions of duplicated 35S promoter, transcriptional start site, hepatitis delta virus antigenomic ribozyme (HDV RZ), and NOS terminator are indicated. **b** Symptoms of *Nicotiana benthamiana* Agro-infiltrated with infectious clone pXT-JaVH^{FJ} and field jasmine sample from Fujian. **c** Detection of genomic RNA, subgenomic RNA and virus derived siRNA of JaVH by Northern blotting and coat protein (CP) by Western blotting. Healthy *N. benthamiana* leaves served as mock and *Jasmine sambac* leaves from Fujian Province containing JaVH served as positive control. A size marker and loading control are shown for reference. **d, e** Characterization of JaVH small RNAs in *J. sambac* (**d**) and *N. benthamiana* (**e**), the frequency of occurrence of each nucleotide at the 5' end, the polarity and the size distribution of small RNAs are presented. **f, g** The distribution of small RNAs mapped to the JaVH genome is presented normalized to reads per million of total small RNAs in *J. sambac* (**f**) and *N. benthamiana* (**g**)

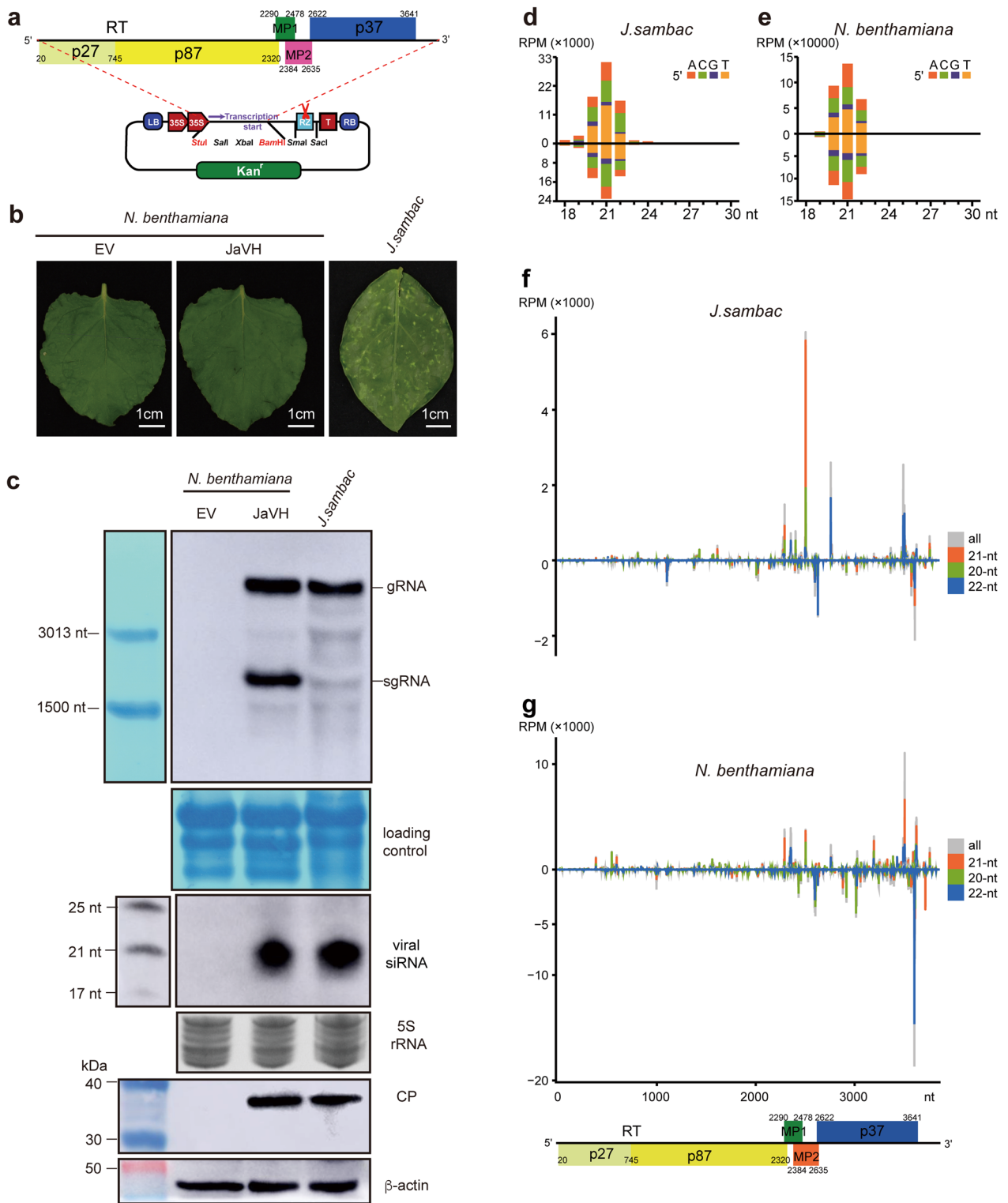


Fig. 1 (See legend on previous page.)

and found that the sgRNA starts at A²²⁶⁸; thus, the sgRNA of JaVH-FJ should be 1600 nt. A protein of the expected size was detected positive using an antiserum raised against viral CP (Zhu et al. 2021) in samples prepared from *N. benthamiana* leaves that were infected with pXT-JaVH^{FJ} and from jasmine leaves collected from the field (Fig. 1c). All the above-mentioned results demonstrate that the amplified clone is indeed an infectious agent in plants.

The small RNA hybridization revealed the presence of virus-derived small RNA, suggesting that JaVH triggers the RNA silencing-mediated antiviral immunity in *N. benthamiana* and *J. sambac* (Fig. 1c). To characterize the virus-derived small RNAs, we constructed two small RNA libraries from newly-collected symptomatic jasmine leaves that were confirmed by RT-PCR with JaVH infection. Similarly, the systemic leaves of *N. benthamiana* Agro-infiltrated with the infectious clone pXT-JaVH^{FJ} were collected (Fig. 1b). The jasmine and *N. benthamiana* libraries contained 9132969 and 21925508 reads, respectively. Of which, 1108332 (~12.1%) and 13532149 (~61.7%) reads were mapped to the JaVH genome, respectively. In both cases, the vast majority of small RNAs were of both polarities with a length of 20-, 21-, and 22-nt, and a predominant peak at 21-nt, which accounted for 42.6% and 42.4% of the total JaVH-FJ derived siRNAs, respectively (Fig. 1d, e). In *Arabidopsis*, the 5'-terminal nucleotides partially determine the preference of AGO proteins for sRNAs (Mi et al. 2008). Therefore, the distribution of 5'-terminal nucleotides was determined with the sequenced JaVH-derived siRNAs. In both cases, there was no significant difference for 5'-terminal nucleotide preference (Fig. 1d, e). Polarity analysis of JaVH-sRNAs showed that they were derived almost equally from the positive-sense genomic sequence (59.3% and 49.1%) and the antisense genomic sequence (40.6% and 50.9%) in *J. sambac* and *N. benthamiana* (Fig. 1d, e). The high density of viral small RNAs allowed a better appreciation of their distribution along the genome and showed two significant hotspots of small RNAs. One was located at the 5' terminus of the predicted sgRNA. The other was located at the 3' terminus of the genome, including the 3' UTR and part of the region encoding CP (Fig. 1f, g). Further analysis of those 18–30-nt JaVH-derived siRNAs showed that, within the JaVH genome, the distribution peaks representing the 21-nt JaVH-derived siRNAs almost overlapped with the peaks representing the 20- and 22-nt JaVH-derived siRNAs (Fig. 1f, g). Based on this result, we concluded that JaVH produced typical small RNAs that are likely processed by a Dicer 4 (DCL4) ortholog and are predominant 21-nt in length, which has been frequently found in many other plant viruses (Szittyá and Burgyán 2013).

pXT-JaVH^{FJ} could systematically infect *J. sambac*

Since no JaVH-free jasmine plants were available, the jasmine seeds were collected and sterilized and virus-free seedlings were cultivated. Healthy jasmine plants were then used for mechanical inoculation with total RNA from *N. benthamiana* that were Agro-infiltrated with pXT-JaVH^{FJ}. Typical yellow spots were observed at two months after inoculation (Fig. 2a) on systemic leaves. To eliminate the possibility that the symptom resulted from the infection of other known jasmine viruses such as jasmine virus T, C, or the newly discovered jasmine virus A (MN915109–MN915111), multiple RT-PCR was performed for detection and only JaVH was detected (Additional file 1: Figure S1). The gRNA, sgRNA, viral derived small RNAs, and CP derived from JaVH detected by Northern and Western blots displayed the expected sizes, which indicates a systematic infection of JaVH in jasmine leaves (Fig. 2b). RT-PCR was performed and subsequent sequencing showed that the amplicon sequences were identical with the infectious clone, pXT-JaVH^{FJ}. The test was performed on 10 jasmine plants, and all 10 plants were systemically infected. Taken together, it can be concluded that pXT-JaVH^{FJ} systematically infected *J. sambac*.

Virus detection and phylogenetic analysis of isolates from different regions

In general, RNA viruses can produce high levels of genetic variation to adapt to new environments. To gain a better understanding of JaVH genetic variation and evolution in different jasmine production areas, samples of jasmine leaves from eight provinces of China, including Jilin (JL), Jiangsu (JS), Sichuan (SC), Shandong (SD), Guangdong (GD), Guangxi (GX), Hunan (HN), and Yunnan (YN) were collected. These samples were first examined for JaVH infection by RT-PCR (primers 360F/800R) and Northern blotting, and positive samples were then confirmed by Western blotting of JaVH CP (Fig. 3a). Full length of JaVH isolates were amplified via RT-PCR and cloned into cloning vectors for sequencing. Subsequently, the complete genomic sequences of eight isolates were determined, which showed that majority of the isolate genomes were comprised of 3867 nts, with the exception of the JL isolate, which had an additional nucleotide in the 3' UTR. Virus isolate names and GenBank accession numbers are shown in Table 1. ORF finder revealed the presence of five ORFs for all isolates, which was consistent with JaVH-FJ.

To determine the phylogenetic relationship of JaVH-FJ to other isolates of JaVH, we aligned the full-length genome sequence of JaVH-FJ with the above eight isolates (Fig. 3b), together with two isolates from Hawaii (HI) and Washington, D.C. (DC), that were reported in 2018 (Dey et al. 2018). Additional phylogenetic trees

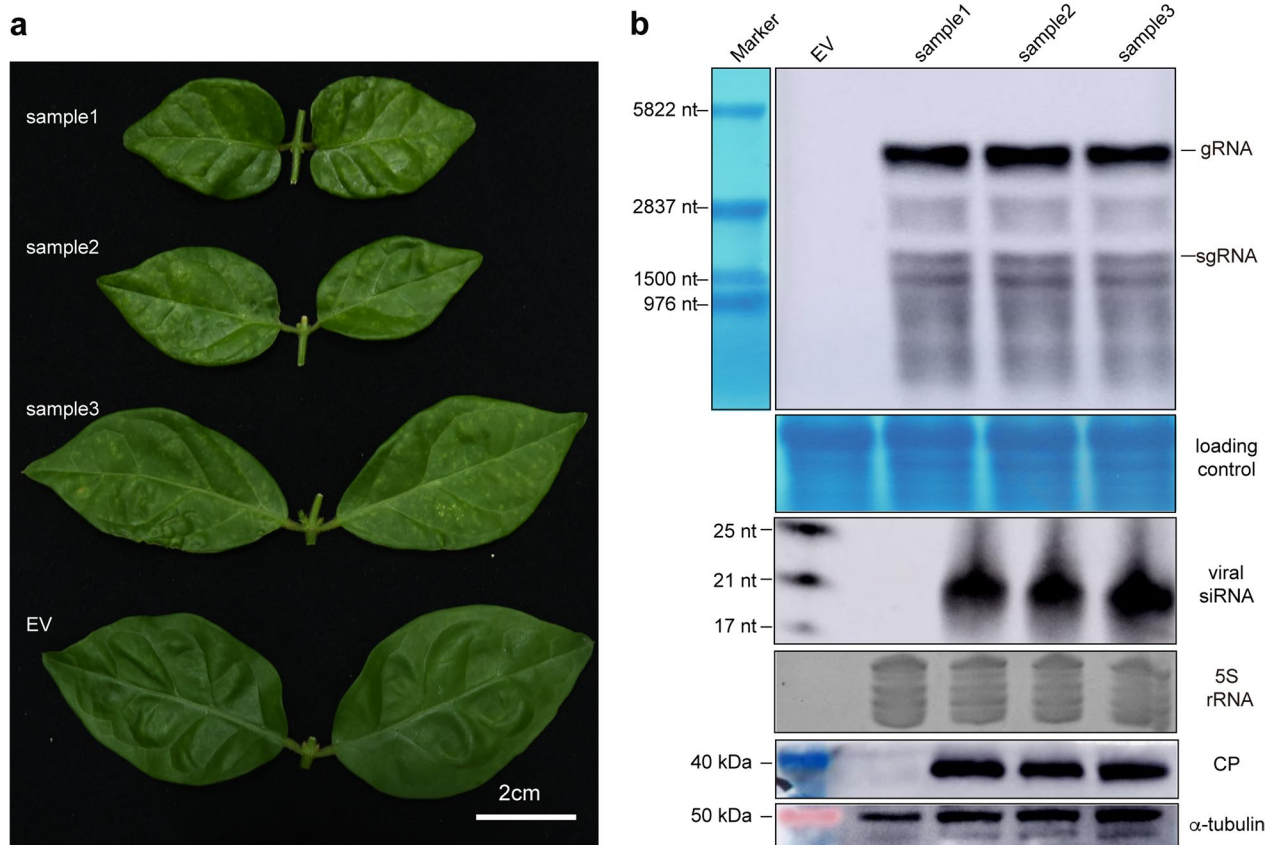


Fig. 2 Symptoms and detection of JaVH in jasmine samples. **a** Typical yellow spots were observed two months after mechanical inoculation with total RNA of Agro-infiltrated *Nicotiana benthamiana*. **b** Detection of genomic RNA, subgenomic RNA, and virus derived siRNA of JaVH by Northern blotting and coat protein by Western blotting. A size marker and loading control are shown for reference

were also constructed using the deduced amino acid sequences of the replicase protein p87 (Fig. 3c). In both phylogenetic analyses, with the exception of JaVH-SC, the 11 isolates fell into four distinct groups: (1) GX, YN, and GD; (2) HN, JS, and SD; (3) FJ and JL; (4) HI and DC. Further pairwise alignments between JaVH-FJ and other isolates were also performed to gain a better understanding of the differences. JaVH-FJ shared 90.2–99.2% nucleotide identity with other isolates (Table 1). The deduced amino acids (p27, p87, MP1, MP2, and CP) identities between JaVH-FJ and the other isolates were 93.8–100%, 96.2–100%, 95.2–100%, 92.8–100%, and 96.8–99.7%,

respectively. Surprisingly, JaVH-JL shared the highest identities in almost every region with JaVH-FJ, except for the 3' UTR (Table 1). Interestingly, 10 of the 11 nucleotide variants between JaVH-FJ and JaVH-JL in coding regions were synonymous differences, with the exception of residue 331 of CP (Ser for JaVH-FJ and Gly for JaVH-JL). The remaining 19 nucleotide variants were located in the 3' UTR (Fig. 3d).

The 3' UTR is critical for the viral RNA accumulation of JaVH
Despite their high sequence similarities, jasmine infected by JaVH-FJ exhibited severer symptoms (Fig. 4a) and

(See figure on next page.)

Fig. 3 JaVH detection in jasmine leaves from different provinces. **a** Western blotting analysis of JaVH CP with *Jasmine sambac* leaves collected from different area of China. FJ, JL, JS, SC, SD, GD, GX, HN, and YN stands for *J. sambac* leaves from Fujian, Jilin, Jiangsu, Sichuan, Shandong, Guangdong, Guangxi, Hunan, and Yunnan provinces, respectively. *Nicotiana benthamiana* leaves Agro-infiltrated with JaVH-FJ and healthy leaves (Mock) are the positive and negative controls, respectively. **b, c** Phylogenetic tree analysis was generated based on the complete genomic nucleotide sequences (**b**) and amino acids of RdRp (**c**) of eleven JaVH isolates. The tree was assembled using MEGA X and the maximum likelihood method (Kumar et al. 2018). Numbers on the nodes indicate the percentage of consistent bootstraps (n = 1000). **d** Nucleotide variants between JaVH-FJ and JaVH-JL. Variants are showed in red or blue color and positions are indicated

Table 1 Percent nucleotide (nt) and amino acid (aa) sequence identity between jasmine virus H Fujian isolate and ten other isolates

Isolate	Accession no	Genomic sequence (nt)	p27 (aa)	p87 (aa)	MP1 (aa)	MP2 (aa)	CP (aa)	3' UTR (nt)
JaVH-GD	MH231175.1	91.6	94.2	97.3	100.0	96.4	97.9	96.0
JaVH-GX	MH231176.1	91.6	93.8	97.1	98.4	96.4	97.9	94.7
JaVH-HN	MH231177.1	91.1	95.0	96.9	96.8	92.8	97.6	96.5
JaVH-JL	MH231178.1	99.2	100.0	100.0	100.0	100.0	99.7	91.6
JaVH-JS	MH231179.1	91.5	95.0	97.3	95.2	92.8	97.9	95.6
JaVH-SC	MH231180.1	92.6	96.3	98.1	98.4	96.4	98.2	95.1
JaVH-SD	MH231181.1	91.5	95.5	97.1	98.4	94.0	97.9	96.9
JaVH-YN	MH231182.1	91.8	94.2	97.5	98.4	95.2	97.3	95.6
JaVH-HI	MG958505.1	90.2	93.8	96.2	96.8	94.0	96.8	92.5
JaVH-DC	MF991299.1	91.7	95.9	96.5	98.4	95.2	97.9	96.0

The lowest similarities are indicated in italics

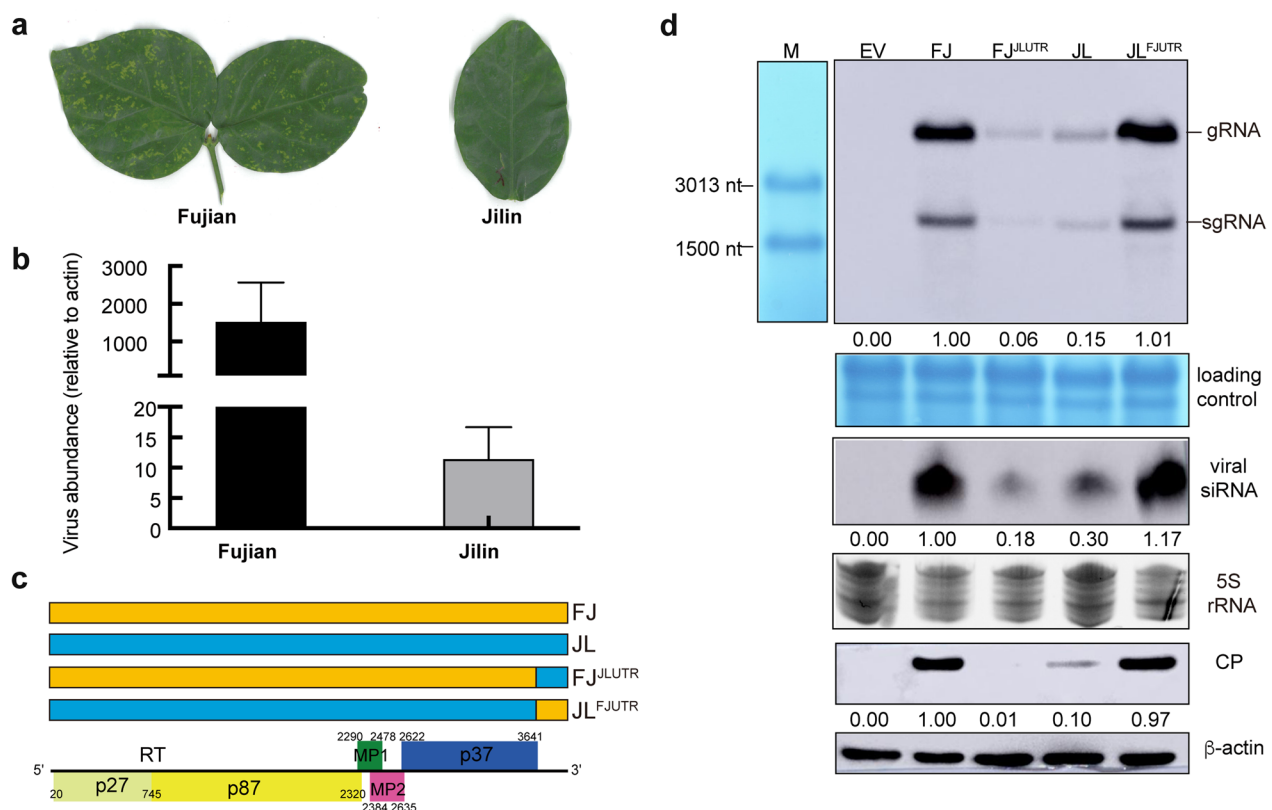


Fig. 4 Pathogenicity assessment of recombinant viruses constructed based on field symptoms difference. **a** Typical mosaic was observed on jasmine samples from Fujian but not Jilin Province. **b** Relative quantification of viral RNA by real time qPCR in jasmine leaves showed in **a**, relative abundance of JaVH was estimated by the $2^{-\Delta CT}$ method using actin as control. **c** Schematic diagram of recombinant plasmids. The yellow box represents sequences related to JaVH-FJ while the blue box represents sequences related to JaVH-JL. **d** Detection of genomic RNA, subgenomic RNA, and virus derived siRNA of JaVH by Northern blotting and CP by Western blotting at 15 days post-infiltration (dpi). A size marker and loading control are shown for reference

higher levels of viral RNA (Fig. 4b) than that infected by JaVH-JL. To clarify the reason for this large difference in viral pathogenicity, an infectious clone sampled from Jilin

Province, pXT-JaVH^{JL}, was constructed and compared with JaVH-FJ to test the viral RNA accumulation in Agrobacterium-infiltrated *N. benthamiana*. The results were consistent

with those of field jasmine samples, where JaVH-JL transcripts accumulated at lower levels relative to JaVH-FJ (Fig. 4d). Considering the high identity between JaVH-FJ and JaVH-JL coding regions, nucleotide variation might be responsible for the difference of their pathogenicity, especially the large number of nucleotide differences in the 3' UTR. To determine the function of the 3' UTR in the course of viral infection, FJ^{JLUTR} were constructed by replacing the complete 3' UTR with that of JL, while JL^{FJUTR} were constructed by replacing the complete 3' UTR with that of FJ (Fig. 4c). Northern blotting results showed that the viral RNA accumulation of FJ^{JLUTR} was much lower than that of FJ, and almost reduced to a level similar to that of JL (Fig. 4d). Comparatively, JL^{FJUTR} with the 3' UTR from FJ recovered the viral RNA accumulation to the level of FJ (Fig. 4d). Collectively, these results indicate that the 3' UTR is critical for the viral RNA accumulation of JaVH.

Discussion

Previously, we reported JaVH as a new member of *Pelarspovirus* (Zhuo et al. 2018). It is well known that the construction of an infectious clone is useful to study viral molecular characterization and function. Thus, JaVH-FJ was constructed in a binary plasmid backbone and Agrobacterium-infiltrated into *N. benthamiana*. The full-length cDNA clone was proved to be infectious in *N. benthamiana* and *J. sambac* (Figs. 1, 2, 4).

RNA silencing is believed to be an evolutionarily conserved antiviral mechanism in many lineages of organisms (Ding 2010), and it is likely that most plants, if not all, encode the arsenal of proteins required for its functioning (Szittyá and Burgyán 2013). In this study, based on the results of small RNA sequencing, we demonstrated that *J. sambac* mounts an RNAi-based antiviral response against JaVH (Fig. 1d–g), although it seems insufficient to halt virus infection, as the virus persists in jasmine plants (Fig. 1b–d). This is likely due to the fact that JaVH encodes p37 (CP) to subvert the antiviral RNAi response of host plants.

Shortly after JaVH was first discovered in Fujian Province of China (Zhuo et al. 2018), Dey et al. (2018) also found the occurrence of JaVH in Hawaii and Washington, D.C. Viruses are well known for their dynamic evolution and rapid adaptation through the accumulation of genome-associated changes and recombination events (Roossinck 1997; Simmonds et al. 2019). Shrubs such as *J. sambac* usually exist for many years, so that after the initial invasion, several recurrent mutations of the virus can be selected and accumulate. Geography-associated evolution seems to be common to plant viruses (Gao et al. 2016). Isolates of JaVH in this study were found to be variable in different geographical area (Fig. 3b, c),

suggesting a geography-associated evolution in JaVH family. However, the phylogenetic tree constructed with whole genome sequence or genome sequence of p87 (RdRp) displayed an unexpected branch of JaVH-SC. Further comparative analyses of JaVH-SC with other isolates did not reveal any recombination events. One possible reason for this notion could be attributed to the field samples collected that were not representative for the entire region of Sichuan Province. Surprisingly, as the naturally occurring pathogens, the coding regions of JaVH-JL were almost identical to JaVH-FJ, although these two isolates exhibit the highest inconformity in the 3' UTR (Fig. 3d).

High-temperature is capable of provoking spontaneous gene mutations in pathogens (Yoon and Chang 2011). With the exception of Jilin isolate, most of the areas that jasmine samples were collected from have summer temperatures exceeding 30°C, implying that temperature may be of importance in the process of JaVH genetic diversification.

Previous studies showed that LDRI can span significant distances within viral RNA genomes, ranging from one to several thousand nucleotides (Miller and White 2006; Nicholson and White 2014; Newburn and White 2015). Viral 3' UTRs play an important role in viral replication and translation through LDRI, and many of which belong to the *Tombusviridae* (Newburn and White 2015; Pyle et al. 2019; Ilyas et al. 2021). Efficient translation of PLPV of the genus *Pelarspovirus* relies on a TED-Like CITE in the 3' UTR that communicates with the corresponding 5'-region through LDRI (Blanco-Pérez et al. 2016). An analysis of RNA secondary structure revealed that a TED-like CITE were also present in JaVH-FJ (Additional file 1: Figure S2b), JL (Additional file 1: Figure S2c) and JL^{FJUTR} (Additional file 1: Figure S2d), but not FJ^{JLUTR} (Additional file 1: Figure S2e) for interaction with 5'-region (Additional file 1: Figure S2a). Given that the presence or absence of a TED-Like CITE in the 3' UTR was not consistent with the accumulation of viruses, it is speculated that the TED-Like CITE was not the main factor responsible for the distinct pathogenicity between JaVH-FJ and JL. Thus, JaVH may use other forms of LDRI to facilitate viral replication.

Conclusions

In this study, we generated a full-length infectious clone of JaVH that was biologically active, and confirmed JaVH as the pathogen associated with the development of yellow mosaic symptoms in jasmine. We also investigated the occurrence and variation of JaVH in the main jasmine-producing areas of China, and revealed that differences in the 3' UTR were closely related to the severity of symptoms.

Methods

Plant materials and growth conditions

Wild type (WT) *N. benthamiana* was grown at $24 \pm 1^\circ\text{C}$ with 60% relative humidity under a 16 h light and 8 h dark cycle. Jasmine samples were collected from fields of Guangdong, Guangxi, Jiangsu, Hunan, Sichuan, and Yunnan provinces of China in the summer of 2016. Samples of Shandong and Jilin provinces were collected from greenhouse.

Inoculation of *J. sambac*

N. benthamiana leaves that were Agro-infiltrated with pXT-JaVH^{FJ} were collected at 15 dpi and total RNA were extracted. 10 μL total RNA with a concentration of 1 $\mu\text{g}/\mu\text{L}$ was inoculated on new leaves with carborundum dusted.

Plasmids construction

Total RNA of jasmine leaves from eight provinces were extracted using hot phenol method (Verwoerd et al. 1989) and used for first-strand cDNA synthesis by the EasyScript[®] Reverse Transcriptase. Samples tested positive for JaVH (primer pair 360F/800R) were then used for full-length amplification (primer pair 001F/JaTo3R) with Phusion[®] High-Fidelity PCR Kit (New England BioLabs, Cat. No. E0553S, USA) by RT-PCR. The resulting fragments were then cloned into pTOPO to generate pTOPO-JaVH-GD, JaVH-GX, JaVH-JL, JaVH-JS, JaVH-HN, JaVH-SC, JaVH-SD, and JaVH-YN, respectively. At least three clones were sequenced to give the complete virus sequences, which were deposited into the NCBI GenBank database under the accession number MH231175.1, MH231176.1, MH231177.1, MH231178.1, MH231179.1, MH231180.1, MH231181.1, and MH231182.1, respectively.

The full-length fragment of JaVH-FJ (NC_055545.1) was amplified by PCR (primer pair 001F/JaTo3R-BamH) using pTOPO-JaVH (Zhuo et al. 2018) as template and then cloned into the *Stu* I and *Bam*H I digested modified pCB301 (Yao et al. 2011) to generate pXT-JaVH^{FJ}. pXT-JaVH^{JL} was generated based on the same strategy using pTOPO-JaVH-JL as template.

Fragment 1 (1–3641 bp) of Fujian isolate amplified with primers XTFJ001F/FJCPutrR and fragment 2 (3642–3868 bp) of Jilin isolate amplified with primers JLCPutrF/XTJLutrR were cloned into the *Stu* I and *Bam*H I digested pCB301 vector (Yao et al. 2011) to generate pXT-FJ^{LU^{TR}} using Gibson Assembly method, according to the manufacturer's instructions (New England BioLabs, Cat. No. E2611S, USA).

Fragment 3 (1–3641 bp) of Jilin isolate amplified with primers XTJL001F/JLCPutrR and fragment 4

(3642–3867 bp) of Fujian isolate amplified with primers FJCPutrF/XTFJutrR were cloned into the *Stu* I and *Bam*H I digested pCB301 vector (Yao et al. 2011) to generate pXT-JL^{FJ^{UTR}} using Gibson Assembly method, according to the manufacturer's instructions (New England BioLabs, Cat. No. E2611S, USA). All clones were confirmed by sequencing. The sequences of all primers used in this study are listed (Additional file 2: Table S1). All restriction enzymes used are from Takara Biomedical Technology (Beijing). *Escherichia coli* strain JM109 was used for the above cloning experiments and all clones were confirmed by sequencing. *A. tumefaciens* GV3101 was used for Agro-infiltration as previously described (Han et al. 2010).

RNA library construction, small RNAs assembly, and downstream sequence analyses

Small RNA Library were constructed as previously described (Zhuo et al. 2018) and sequenced in an Illumina HiSeq 2500 instrument (Novogen, China). Sequencing adapters were trimmed with in-house Perl scripts. Small RNAs were assembled into contigs using MetaVelvet (Namiki et al. 2012). Resulting contigs were aligned to the 'nr' protein database of NCBI using the BLASTx algorithm. After recovery of the whole sequence of the virus by RACE, small RNAs were mapped on the sequence using Bowtie (Langmead et al. 2009) and the results were parsed with Perl scripts. Plots were generated in R. The sequences of libraries described in this article are publicly available at the GEO portal of NCBI and can be found in the GEO accession portal under the accession number GSE96704.

Northern blotting

To detect genomic RNAs, total RNA (5 μg) extracted from *N. benthamiana* was separated by electrophoresis in a 1.2% (w/v) agarose-formaldehyde gel and transferred to a Hybond-N + membrane (GE Amersham, Cat. No. RPN303B, USA) by capillary transfer. The membrane was cross-linked by UV and stained with methylene blue to assess loading control. The membrane was then hybridized with a DIG-dUTP-labeled JaVH-specific DNA probe (nts 3642–3867) prepared by random priming according to the manufacturer's instructions (Roche, Cat. No. 11585606910, Switzerland).

Northern blotting of small RNAs was carried out as previously described with minor changes (Han et al. 2011). Briefly, low molecular weight (LMW) RNAs (5 μg) obtained after LiCl and isopropanol precipitation were fractionated on a denaturing 15% polyacrylamide gel containing 8 mol/L urea, electroblotted onto Hybond-NX membranes (GE Amersham, Cat. No. RPN303T, USA), chemically

cross-linked (Sigma-Aldrich, Cat No. E7750, USA), and hybridized with DIG-dUTP-labeled JaVH-specific LNA oligonucleotides. LNA probes were designed based on top reads of small RNA libraries complementary to either the positive (TGCA+GAGTA+CGATGC+AGATC,+stands for LNA modification) or the negative strands (AGAA+AACTA+GTCTAC+GTCTG,+stands for LNA modification) and prepared by end tailing according to the manufacturer's instructions (Roche, Cat. No. 03353583910, Switzerland). 5S rRNA stained with nucleic acid dye was used as loading control. The membrane was then hybridized at 42°C overnight with the above probe in PerfectHyb™ Plus Hybridization Buffer (Sigma, Cat No. H7033, USA).

Detection of hybridized material was conducted with the CSPD ready-to-use reagents (Roche, Cat No. 000000011655884001, Switzerland). Chemiluminescent signals were collected in an Imager 600 (GE Amersham, USA).

Western blotting

Proteins were extracted as described by Wang et al. (2003) and finally resuspended in 8 mol/L urea solution including 1% SDS (Simon and Miller 2013). Proteins were fractionated by SDS-PAGE and transferred to nitrocellulose filters (MERCCK, Cat. No. HATF0000, USA). Filters were blocked overnight at 4°C in TBS-T buffer (10 mM Tris-HCl [pH 8.0], 150 mM NaCl, 0.05% Tween 20) containing 3% Bovine Serum Albumin (BSA, Solarbio, Cat. No. A8020, China). Proteins were detected using a rabbit polyclonal antiserum raised against the coat protein (Zhu et al. 2021) or a monoclonal anti α -tubulin antibody (Sigma, Cat. No. T6074, USA) or β -actin (Labeled, Cat No. BP0101, Beijing, China). Membranes were then incubated with secondary goat anti-rabbit/mouse immunoglobulin G conjugated to horseradish peroxidase (Sigma, Cat. No. A0545/A90044, USA) and finally detected using ECL reagents (Bio-Rad, Cat. No. 1705062S, USA). Chemiluminescence signals were collected using an Imager 600.

Reverse transcription PCR

Total RNA was extracted from leaves and then reverse transcribed according to the manufacturer's instructions (Promega, Cat. No.0000380555, USA). PCR was then carried out with 2 × Taq Master Mix (Vazyme, Cat. No. P112-01, USA) using virus specific primers in Additional file 2: Table S1.

Quantitative real-time PCR

Total RNA was extracted from jasmine leaves. cDNAs were synthesized by using First-strand cDNA synthesis

supermix (TransGen Biotech, Cat. No. AT341, China). Real-time quantitative PCR was carried out in the presence of SYBR green Supermix (TransGen Biotech, Cat. No. AQ131, China). The relative abundance of JaVH were normalized to an internal control (actin). Primers used are showed in Additional file 2: Table S1. Relative abundance was estimated by the Δ CT method (Han et al. 2011).

Abbreviations

3' UTR	3'-Untranslated region
aa	Amino acid
BBSV	Beet black scorch virus
BSA	Bovine serum albumin
cDNA	Complementary DNA
CITEs	Cap-independent translational enhancers
CP	Coat protein
DC	Washington D.C.
DCL4	Dicer 4
<i>N. benthamiana</i>	<i>Nicotiana benthamiana</i>
GD	Guangdong
gRNA	Genomic RNA
GX	Guangxi
HDV RZ	Hepatitis delta virus antigenomic ribozyme
HI	Hawaii
HN	Hunan
<i>J. sambac</i>	<i>Jasminum sambac</i>
dpi	Days post-infiltration
JaVH	Jasmine virus H
JL	Jilin
JS	Jiangsu
LDRIIs	Long-distance RNA-RNA interactions
LMW	Low molecular weight
nts	Nucleotides
ORFs	Open reading frames
PLPV	Pelargonium line pattern virus
RACE	Rapid amplification of cDNA end
RCNMV	Red clover necrotic mosaic virus
RT-PCR	Reverse transcription-polymerase chain reaction
SC	Sichuan
SD	Shandong
sgRNA	Subgenomic RNA
siRNAs	Small interfering RNAs
sRNAs	Small RNAs
TCV	Turnip crinkle virus
TED	Translation enhancer domain
TSS	TRNA-shaped structure
UTR	Untranslated region
VSR	Viral suppressor of RNA silencing
WT	Wild type
YN	Yunnan

Supplementary Information

The online version contains supplementary material available at <https://doi.org/10.1186/s42483-023-00161-5>.

Additional file 1: Figure S1. Virus detection by RT-PCR of jasmine samples inoculated with total RNA of Agro-infiltrated *Nicotiana benthamiana*. **Figure S2.** Putative secondary structure predicted in JaVH isolates and recombinant viruses.

Additional file 2: Table S1. Primers used in this study.

Acknowledgements

We thank Dr. Xiaorong Tao (Nanjing Agricultural University) for providing pXT vector. We thank International Science Editing (<http://www.international-scienceediting.com>) for editing this manuscript.

Authors' contributions

YH designed the research. LZ, CZ, YB, SH, CJ, and QC performed the research. YH and QX analyzed the data and wrote the manuscript. All authors read and approved the final manuscript.

Funding

This work was supported by the National Natural Science Foundation of China (Grant No. 31900153 to YH), Natural Science Foundation of Fujian Province (Grant No. 2017J01600 to YH), and Fujian Agriculture and Forestry University (FAFU) Construction Project for Technological Innovation and Service System of Tea Industry Chain (K1520005A02).

Availability of data and materials

Not applicable.

Declarations

Ethics approval and consent to participate

Not applicable.

Consent for publication

Not applicable.

Competing interests

The authors declare that they have no competing interests.

Received: 28 September 2022 Accepted: 17 January 2023

Published online: 21 February 2023

References

- An M, Iwakawa HO, Mine A, Kaido M, Mise K, Okuno T. A Y-shaped RNA structure in the 3' untranslated region together with the trans-activator and core promoter of red clover necrotic mosaic virus RNA2 is required for its negative-strand RNA synthesis. *Virology*. 2010;405:100–9. <https://doi.org/10.1016/j.virol.2010.05.022>.
- Blanco-Pérez M, Pérez-Cañamás M, Ruiz L, Hernandez C. Efficient translation of pelargonium line pattern virus RNAs relies on a TED-like 3'-translational enhancer that communicates with the corresponding 5'-region through a long-distance RNA-RNA interaction. *PLoS ONE*. 2016;11:e152593. <https://doi.org/10.1371/journal.pone.0152593>.
- Castano A, Ruiz L, Hernández C. Insights into the translational regulation of biologically active open reading frames of pelargonium line pattern virus. *Virology*. 2009;386:417–26. <https://doi.org/10.1016/j.virol.2009.01.017>.
- Dey KK, Leite M, Hu JS, Jordan R, Melzer MJ. Detection of jasmine virus H and characterization of a second pelarspovirus infecting star jasmine (*Jasminum multiflorum*) and angelwing jasmine (*J. nitidum*) plants displaying virus-like symptoms. *Arch Virol*. 2018;163:3051–8. <https://doi.org/10.1007/s00705-018-3947-y>.
- Ding SW. RNA-based antiviral immunity. *Nat Rev Immunol*. 2010;10:632–44. <https://doi.org/10.1038/nri2824>.
- Dreher TW, Miller WA. Translational control in positive strand RNA plant viruses. *Virology*. 2006;344:185–97. <https://doi.org/10.1016/j.virol.2005.09.031>.
- Fabian MR, White KA. 5'–3' RNA-RNA interaction facilitates cap- and poly(A) tail-independent translation of tomato bushy stunt virus mRNA: a potential common mechanism for *tombusviridae*. *J Biol Chem*. 2004;279:28862–72. <https://doi.org/10.1074/jbc.M401272200>.
- Firth AE, Brierley I. Non-canonical translation in RNA viruses. *J Gen Virol*. 2012;93:1385–409. <https://doi.org/10.1099/vir.0.042499-0>.
- Gao F, Jin J, Zou W, Liao F, Shen J. Geographically driven adaptation of chilli veinal mottle virus revealed by genetic diversity analysis of the coat protein gene. *Arch Virol*. 2016;161:1329–33. <https://doi.org/10.1007/s00705-016-2761-7>.
- Han YH, Xiang HY, Wang Q, Li YY, Wu WQ, Han CG, et al. Ring structure amino acids affect the suppressor activity of melon aphid-borne yellows virus P0 protein. *Virology*. 2010;406:21–7. <https://doi.org/10.1016/j.virol.2010.06.045>.
- Han YH, Luo YJ, Wu Q, Jovel J, Wang XH, Aliyari R, et al. RNA-based immunity terminates viral infection in adult *Drosophila* in the absence of viral suppression of RNA interference: characterization of viral small interfering RNA populations in wild-type and mutant flies. *J Virol*. 2011;85:13153–63. <https://doi.org/10.1128/JVI.05518-11>.
- Ilyas M, Du Z, Simon AE. Opium poppy mosaic virus has an xrn-resistant, translated subgenomic RNA and a BTE 3' CITE. *J Virol*. 2021. <https://doi.org/10.1128/JVI.02109-20>.
- Jiang Y, Li Z, Nagy PD. Nucleolin/Nsr1p binds to the 3' noncoding region of the tombusvirus RNA and inhibits replication. *Virology*. 2010;396:10–20. <https://doi.org/10.1016/j.virol.2009.10.007>.
- Kneller EL, Rakotondrafara AM, Miller WA. Cap-independent translation of plant viral RNAs. *Virus Res*. 2006;119:63–75. <https://doi.org/10.1016/j.virusres.2005.10.010>.
- Kumar S, Stecher G, Li M, Niyaz C, Tamara K. MEGA X: molecular evolutionary genetics analysis across computing platforms. *Mol Biol Evol*. 2018;35:1547–9. <https://doi.org/10.1093/molbev/msy096>.
- Langmead B, Trapnell C, Pop M, Salzberg SL. Ultrafast and memory-efficient alignment of short DNA sequences to the human genome. *Genome Biol*. 2009;10:R25. <https://doi.org/10.1186/gb-2009-10-3-r25>.
- Mi S, Cai T, Hu Y, Chen Y, Hodges E, Ni F, et al. Sorting of small RNAs into *Arabidopsis* argonaute complexes is directed by the 5' terminal nucleotide. *Cell*. 2008;133:116–27. <https://doi.org/10.1016/j.cell.2008.02.034>.
- Miller WA, White KA. Long-distance RNA-RNA interactions in plant virus gene expression and replication. *Annu Rev Phytopathol*. 2006;44:447–67. <https://doi.org/10.1146/annurev.phyto.44.070505.143353>.
- Namiki T, Hachiya T, Tanaka H, Sakakibara Y. MetaVelvet: an extension of velvet assembler to de novo metagenome assembly from short sequence reads. *Nucleic Acids Res*. 2012;40:e155. <https://doi.org/10.1093/nar/gks678>.
- Newburn LR, White KA. Cis-acting RNA elements in positive-strand RNA plant virus genomes. *Virology*. 2015;479–480:434–43. <https://doi.org/10.1016/j.virol.2015.02.032>.
- Nicholson BL, White KA. 3' Cap-independent translation enhancers of positive-strand RNA plant viruses. *Curr Opin Virol*. 2011;1:373–80. <https://doi.org/10.1016/j.coviro.2011.10.002>.
- Nicholson BL, White KA. Functional long-range RNA-RNA interactions in positive-strand RNA viruses. *Nat Rev Microbiol*. 2014;12:493–504. <https://doi.org/10.1038/nrmicro3288>.
- Pérez-Cañamás M, Hernández C. Key importance of small RNA binding for the activity of a glycine-tryptophan (GW) motif-containing viral suppressor of RNA silencing. *J Biol Chem*. 2015;290:3106–20. <https://doi.org/10.1074/jbc.M114.593707>.
- Pérez-Cañamás M, Hernández C. New insights into the nucleolar localization of a plant RNA virus-encoded protein that acts in both RNA packaging and RNA silencing suppression: involvement of importins alpha and relevance for viral infection. *Mol Plant Microbe Interact*. 2018;31:1134–44. <https://doi.org/10.1094/MPMI-02-18-0050-R>.
- Pyle JD, Mandadi KK, Scholthof K. Panicum mosaic virus and its satellites acquire RNA modifications associated with host-mediated antiviral degradation. *Mbio*. 2019. <https://doi.org/10.1128/mBio.01900-19>.
- Roossinck MJ. Mechanisms of plant virus evolution. *Annu Rev Phytopathol*. 1997;35:191–209. <https://doi.org/10.1146/annurev.phyto.35.1.191>.
- Scheets K, Jordan R, White KA, Hernandez C. *Pelarspovirus*, a proposed new genus in the family *Tombusviridae*. *Arch Virol*. 2015;160:2385–93. <https://doi.org/10.1007/s00705-015-2500-5>.
- Simmonds P, Aiewsakun P, Katzourakis A. Reply to 'evolutionary stasis of viruses?' *Nat Rev Microbiol*. 2019;17:329–30. <https://doi.org/10.1038/s41579-019-0169-6>.
- Simon AE. 3' UTRs of carmoviruses. *Virus Res*. 2015;206:27–36. <https://doi.org/10.1016/j.virusres.2015.01.023>.
- Simon AE, Miller WA. 3' cap-independent translation enhancers of plant viruses. *Annu Rev Microbiol*. 2013;67:21–42. <https://doi.org/10.1146/annurev-micro-092412-155609>.
- Szittya G, Burgyn J. RNA interference-mediated intrinsic antiviral immunity in plants. *Curr Top Microbiol Immunol*. 2013;371:153–81. https://doi.org/10.1007/978-3-642-37765-5_6.

- Verwoerd TC, Dekker BM, Hoekema A. A small-scale procedure for the rapid isolation of plant RNAs. *Nucleic Acids Res.* 1989;17:2362. <https://doi.org/10.1093/nar/17.6.2362>.
- Wang W, Scali M, Vignani R, Spadafora A, Sensi E, Mazzuca S, et al. Protein extraction for two-dimensional electrophoresis from olive leaf, a plant tissue containing high levels of interfering compounds. *Electrophoresis.* 2003;24:2369–75. <https://doi.org/10.1002/elps.200305500>.
- Xu J, Wang X, Shi L, Zhou Y, Li D, Han C, et al. Two distinct sites are essential for virulent infection and support of variant satellite RNA replication in spontaneous beet black scorch virus variants. *J Gen Virol.* 2012;93:2718–28. <https://doi.org/10.1099/vir.0.045641-0>.
- Yao M, Zhang TQ, Tian ZC, Wang TC, Tao XR. Construction of *Agrobacterium*-mediated cucumber mosaic virus infectious cDNA clones and 2b deletion viral vector. *Sci Agric Sin.* 2011;44:3060–8. <https://doi.org/10.3864/j.issn.0578-1752.2011.14.024>. (in Chinese).
- Yoon BH, Chang HI. Complete genomic sequence of the *Lactobacillus* temperate phage LF1. *Arch Virol.* 2011;156:1909–12. <https://doi.org/10.1007/s00705-011-1082-0>.
- Yuan X, Shi K, Simon AE. A local, interactive network of 3' RNA elements supports translation and replication of turnip crinkle virus. *J Virol.* 2012;86:4065–81. <https://doi.org/10.1128/JVI.07019-11>.
- Zhu LJ, Jiang CY, Han YH. Cloning, prokaryotic expression and antiserum preparation of coat protein gene. *Acta Phytopathol Sin.* 2021;51:654–7. <https://doi.org/10.13926/j.cnki.apps.000533>. (in Chinese).
- Zhu LJ, Zhang CT, Wang YW, Jiang CY, Xie XY, Bai YN, et al. Identification of key residues affecting RNA silencing suppressor activity of jasmine virus H. *J Fujian Agric for Uni (nat Sci Ed).* 2022;51:27–32. [https://doi.org/10.13323/j.cnki.j.fafu\(nat.sci\).2022.01.004](https://doi.org/10.13323/j.cnki.j.fafu(nat.sci).2022.01.004). (in Chinese).
- Zhuo T, Zhu LJ, Lu CC, Jiang CY, Chen ZY, Zhang G, et al. Complete nucleotide sequence of jasmine virus H, a new member of the family *Tombusviridae*. *Arch Virol.* 2018;163:731–5. <https://doi.org/10.1007/s00705-017-3663-z>.

Ready to submit your research? Choose BMC and benefit from:

- fast, convenient online submission
- thorough peer review by experienced researchers in your field
- rapid publication on acceptance
- support for research data, including large and complex data types
- gold Open Access which fosters wider collaboration and increased citations
- maximum visibility for your research: over 100M website views per year

At BMC, research is always in progress.

Learn more biomedcentral.com/submissions

